

# Placement of wind and solar based DGs in distribution system for power loss minimization and voltage stability improvement



Partha Kayal<sup>a,\*</sup>, C.K. Chanda<sup>b</sup>

<sup>a</sup> Department of Electrical Engineering, Future Institute of Engineering and Management, Kolkata 700 150, India

<sup>b</sup> Department of Electrical Engineering, Bengal Engineering and Science University, Shibpur, Howrah 711 103, India

## ARTICLE INFO

### Article history:

Received 14 January 2013

Received in revised form 24 May 2013

Accepted 29 May 2013

### Keywords:

Distributed generation

PSO method

Voltage stability factor

Optimal location

Power losses

## ABSTRACT

Proper placement of Distributed Generation (DG) in distribution system is still very challenging issue for obtaining their maximum potential benefits. This paper proposes a new constrained multi-objective Particle Swarm Optimization (PSO) based Wind Turbine Generation Unit (WTGU) and photovoltaic (PV) array placement approach for power loss reduction and voltage stability improvement of radial distribution system. The paper reflects the effectiveness of WTGU and PV array performance models in DG placement problem formulation. Wind and solar based DGs are operated in different active and reactive power mode and tested on 12-bus, 15-bus, 33-bus and 69-bus radial distribution system. Obtained results are compared with other DG placement technique and proposed method is found to be more effective in terms of voltage stability enhancement and power loss minimization. A novel Voltage Stability Factor (VSF) has been proposed in this paper which can quantify voltage stability levels of buses in the system. Comparing with other voltage stability index and power stability index, developed VSF has emerged as more simple and efficient tool.

© 2013 Elsevier Ltd. All rights reserved.

## 1. Introduction

With growing load demand in the distribution network, it provides potential scope for research in terms of analyzing the distribution network to meet the demand with the present infrastructure. Shortage of distribution current carrying capabilities and increased interest in application of green technology has led to use of Distributed Generation (DG). DG is small-scale power generation that is usually embedded in the distribution system [1]. DG units are mainly energized by wind, solar and fuel cell. There are a number of DG technologies available in the market today and a few are still at the research and development stage. Among available technologies, wind and solar based DG technologies are going to dominate the electricity market because of their environmental friendly characteristics and abundant availability of resources.

Normally the structure of distribution system is radial in nature because of their simplicity. Radial distribution system has main feeders and lateral distributors. The main feeder originates from substation and passes through different consumer loads. Most of the radial distribution system suffers with high power losses because of high resistance to reactance ratios. The overall efficiency

of the system can be improved using DG units. It is important to determine the optimal location for sitting of DGs. DG devices can be strategically placed in power systems for grid reinforcement, reducing power losses and on-peak operating costs, improving voltage profiles and load factors, deferring or eliminating for system upgrades, and improving system integrity, reliability, and efficiency. Installing DG units at non-optimal places may result in an increase in system losses, implying an increase in costs, and therefore, having an opposite effect to what is desired. Moreover, if multiple DG units are installed, optimal approach for placement of DGs in order to maintain the stability and reliability of the system become more crucial. In case of installation of multiple DGs, the problems of optimal placement and sizing of DGs are normally solved by optimization techniques such as Mixed Integer Non-Linear Programming (MINLP), Evolutionary Programming (EP), Differential Evolution (DE), Genetic Algorithm (GA), Particle Swarm Optimization (PSO) technique [3,9–14].

Placement technique of DG units into existing distribution system is a very important aspect of DG planning. Optimal allocation of DGs depends on the choice of objective(s) that need to be fulfilling some goal set by system designers. However, the systematic and cardinal rule for this issue is still an open question.

Acharya et al. [2] have derived a methodology to calculate appropriate optimum location for DG to minimize distribution losses. The methodology is based on exact loss formula. The methodology has been tested with varying size of DG. Singh and Parida

\* Corresponding author. Tel.: +91 3324345640.

E-mail addresses: [partha\\_kayal@yahoo.co.in](mailto:partha_kayal@yahoo.co.in) (P. Kayal), [ckc\\_math@yahoo.com](mailto:ckc_math@yahoo.com) (C.K. Chanda).

[3] have considered cost as an objective function to place solar, wind and fuel cell based DGs. MINLP technique is used to locate DGs optimally. Analytic hierarchy process has been used to make a decision over getting the optimal locations for different kinds of DGs. Kashem and Ledwich [4] have discussed about reinforcement of distribution voltages installing DGs. They have suggested voltage sensitivity based installation of DGs. Network issues that may occur during multiple VSDG inclusion in the network are also studied. A method for placement of DG has been proposed by Hedayati et al. [5]. This method is based on the analysis of power flow continuation and determination of most sensitive buses to voltage collapse. The method aims to minimize power losses and maximize voltage stability margin of the system. Unfortunately multiple DGs cannot be accommodated at a time with this method. To investigate different parameters of the system for installation of multiple DGs, multi objective optimization technique is essential. Lee and Park [6] have determined location of DG based on minimization of network power losses. Optimal size of DG is determined using Kalman filter algorithm. Gonzalez et al. [7] have introduced a hybrid PSO and optimal power flow method for optimal placement and sizing of DG considering the objectives of DG cost and power loss minimization issue. Some constraints like bus voltage limit, thermal limit of lines and transformer, operation and planning limits are imposed on the optimization problem. Wang and Nehrir have discussed analytical approach for optimal placement of DG in the network [8]. DG is placed one by one in the network to obtain minimum power loss of the system. Khatod et al. [9] presented an EP based technique for the optimal placement of DG units. They have also dealt with sensitivity analysis for location selection of DG. A power loss minimization based approach have discussed by authors in [10] for optimal sitting and sizing of DG. Singh et al. [12] have presented a GA based multi objective approach considering power loss indices and voltage profile indices. Sedighi et al. [13] have proposed a method for sitting and sizing of DG considering the objectives of network loss reduction and total harmonic distortion reduction of distribution network. They have used conventional weighted aggregation based multi objective PSO approach which may lead to non-optimal solution in some cases. A methodology has been proposed for optimally allocating different types of renewable Distributed Generation (DG) units in the distribution system [14]. The problem is formulated as MINLP, with an objective function for minimizing the system's annual energy losses. In this approach a few load buses have been considered for allocating DGs. An analytical approach for placement and sizing of DG unit on view point of system power loss minimization has been proposed by Gozel and Hocaoglu [15]. A loss sensitivity factor based on the equivalent current injection is for the determination of the optimum size and location of distributed generation. A DG placement problem is solved based on voltage stability analysis as a security measure by Etehadhi et al. [16]. Sizing of multiple DGs are evaluated based on power loss minimization by Ugral and Karatepe [17]. They have also considered uncertainty of load in their study. Modal analysis and continuous power flow are used in a hierarchal placement algorithm. In [18], the authors have discussed about Power Stability Index (PSI) based DG placement technique. In this technique, PSI value was calculated for each line and sorted from highest to lowest value. DG was placed at bus terminating the highest PSI branch (i.e. most weak voltage stable bus). PSI value was recalculated and in the same manner location for next DG was selected. A loss sensitivity based DG placement approach has been discussed in [19]. The authors have adopted bus ranking method based on loss sensitivity and DGs are placed at high loss sensitive buses. In [20], the authors have discussed an approach for allocation of DG considering the objective function as an algebraic sum of DG cost and product of weighting factor and network power loss. With varying weighting factor, different values of

objective functions are calculated for different buses and DG was proposed to be located at minimum value of objective function. But, in case of multiple DG allocation, the scenario supposed to be different. Ganguly et al. [21] have presented a multi-objective planning approach for electrical distribution systems incorporating DG. The two objectives, minimization of total installation and operational costs, and minimization of the risk factor have been taken into account for system planning. The optimal number and location of the DG units are determined in planning stage. The two objective functions considered in this DG planning optimization are total real power loss and the DG penetration index. Kumar and Banerjee [22] have studied about sizing and sitting of PV module and biomass gasifier based DG in isolated power system. They have used continuation power flow method to place DG considering the objective of distribution loss reduction. In [23] authors have discussed optimal capacitor placement in distribution system considering voltage stability. Aman et al. [24] have discussed about optimal placement of DG on view point of power loss reduction and voltage stability improvement of distribution system. They have used PSO technique with equal weighted sum of two different objectives to find out location and size of DG. Optimal size and location of single DG unit in different distribution systems are presented in the paper.

This paper introduces a multi objective constrained PSO based approach to place DG units for optimal power loss reduction and voltage stability improvement of distribution network. The paper is organized as follows. In first section, some of available voltage stability index along with developed Voltage Stability Factor (VSF) are discussed. Second section is composed of performance modeling of wind and solar power generation system. In third section, Dynamic Weighted Aggregation (DWA) technique is applied on PSO to obtain multi objective PSO. Procedure to select appropriate locations for DG units using PSO method is also presented. Section 5 is divided in two parts. In first part, effectiveness of the proposed VSF is tested on different types of distribution systems. In second part, DG placement technique is experimented on 12-bus, 15-bus, 33-bus and 69-bus radial distribution network and obtained results are discussed. Finally some relevant conclusions are drawn.

## 2. Formulation of voltage stability measurement

Voltage stability has become a major concern in modern power system scenario. The threshold point of voltage stability is determined from voltage stability analysis. Some techniques, i.e. nose curve technique, V-Q sensitivity analysis, Voltage Stability Index (VSI) are helpful to measure voltage stability of the system or to find out critical buses in the network. Among different techniques, VSI based method has emerged as very fast and effective tool for off-line voltage stability analysis. Some voltage stability index and useful formulas proposed by different authors to examine the system stability and thus voltage collapse are described below.

### 2.1. VSI by Jasmon

Jasmon and Lee [25] have derived a VSI which can measure stability of load buses in a power system and represented as follows

$$L_{i+1} = \frac{4 \left[ V_i^2 (P_{i+1} * r_i + Q_{i+1} * x_i) + (P_{i+1} * x_i - Q_{i+1} * r_i)^2 \right]}{V_i^4} \quad (1)$$

where a branch with impedance of  $r_i + jx_i$  is connected between sending end bus with voltage of  $V_i$  and receiving node with loading of  $P_{i+1} + jQ_{i+1}$ .

In [26], authors measured voltage stability of total network by reduced single line method and index by Jasmon was reproduced as

$$L = 4 \left[ (P_{leq} * r_{eq} + Q_{leq} * x_{eq}) + (P_{leq} * x_{eq} - Q_{leq} * r_{eq})^2 \right] \quad (2)$$

where  $P_{leq} + jQ_{leq}$  is the total load and  $r_{eq} + jx_{eq}$  is impedance of connecting branch of reduced single line network.

The authors have concluded that the more the value of VSI nearer to zero signifies more voltage stable operation.

### 2.2. VSI by Shin

In [27], Shin et al. have formulated a VSI from a simple power system with two buses and later the developed VSI is applied on large system with many buses. The developed VSI to asses voltage stability of general radial distribution network was defined as

$$VSI = 0.5 * V_1 - (P_{leq} * r_{eq} + Q_{leq} * x_{eq}) / V_1 \quad (3)$$

where  $V_1$  is the sending end voltage of reduced single line network.

Authors have identified that approaching of VSI towards zero can result voltage collapse by transferring power at critical point through the distribution line.

### 2.3. PSI by Aman

Considering stable node voltages, Aman et al. [18] have formulated a stability index which they have referred as Power Stability Index (PSI). The proposed PSI can identify the critical buses in the system which may face voltage collapse at the time of increased load demand. The PSI for Bus- $j$  is given as

$$PSI_j = \frac{4r_{ij}(P_{Lj} - P_{Gj})}{[|V_i| \cos(\theta_{ij} - \delta_i)]^2} \quad (4)$$

where line of impedance  $|r_{ij} + jx_{ij}| \angle \theta_{ij}$  is connected between Bus- $i$  and Bus- $j$ . Bus- $j$  have total active power load of  $P_{Lj}$  and total active power generation of  $P_{Gj}$ .

The authors have examined that closer the value of PSI to zero, the system would become more stable.

### 2.4. Proposed VSF

A novel technique for determination of voltage stability is discussed in detail here.

Considering two bus section of distribution system of Fig. 1, branch current of any branch 'i' can be obtained as follows.

$$I_i^2 = \left( \frac{P_{m+1}^2 + Q_{m+1}^2}{V_{m+1}^2} \right) \quad (5)$$

where  $P_{m+1}$ ,  $Q_{m+1}$  and  $V_{m+1}$  are the active load, reactive load and bus voltage magnitude at bus 'm + 1'.

So, active and reactive power losses in the branch are given by

$$P_{loss_i} = r_i \left( \frac{P_{m+1}^2 + Q_{m+1}^2}{V_{m+1}^2} \right) \quad (6)$$

$$Q_{loss_i} = x_i \left( \frac{P_{m+1}^2 + Q_{m+1}^2}{V_{m+1}^2} \right) \quad (7)$$

Here  $P_{loss_i}$  and  $Q_{loss_i}$  are the active and reactive power losses of branch 'i'.

$$I_i^2 = \frac{P_{loss_i}^2 + Q_{loss_i}^2}{(V_m - V_{m+1})^2} \quad (8)$$

From (5) and (8), equating  $I_i^2$  it becomes

$$\frac{P_{m+1}^2 + Q_{m+1}^2}{V_{m+1}^2} = \frac{P_{loss_i}^2 + Q_{loss_i}^2}{(V_m - V_{m+1})^2} \quad (9)$$

Putting the value of  $P_{loss_i}$  and  $Q_{loss_i}$  in (9)

$$(P_{m+1}^2 + Q_{m+1}^2) \cdot (r_i^2 + x_i^2) = (V_{m+1}^2 - V_{m+1} \cdot V_m)^2 \quad (10)$$

Taking the positive root of (10)

$$S_{m+1} = \left( \frac{V_{m+1}^2 - V_{m+1} \cdot V_m}{Z_i} \right) \quad (11)$$

$S_{m+1}$  is the magnitude of complex power at receiving end.

For critical power flowing at receiving end

$$\frac{dS_{m+1}}{dV_{m+1}} = \left( \frac{V_{m+1}^2 - V_{m+1} \cdot V_m}{Z_i} \right) = 0 \quad (12)$$

For stable operation of the system

$$\frac{dS_{m+1}}{dV_{m+1}} > 0 \quad \text{i.e.} (2V_{m+1} - V_m) > 0 \quad (13)$$

Voltage stability factor for any bus 'm + 1' is designated as

$$VSF_{m+1} = (2V_{m+1} - V_m) \quad (14)$$

At voltage collapse point VSF will become zero and that will be occurred when magnitude receiving end bus voltage become half of magnitude of sending end bus voltage. The more the value of the VSF nearer to zero, the system is more vulnerable.

Voltage stability condition of the whole distribution system can be justified summing the values of VSF of all the load buses.

So,

$$VSF_{total} = \sum_{m=1}^{k-1} (2V_{m+1} - V_m) \quad (15)$$

'k' is the total number of buses in the system and  $V_1$  is the magnitude of substation voltage. The higher value of  $VSF_{total}$  indicates more voltage stable operation.

## 3. Performance modeling of wind and solar generation system

Power generation of Wind Turbine Generation Unit (WTGU) and PV array depends on their model and resource such as wind speed, solar radiation and ambient temperature. In this section modeling of WTGU and PV array is discussed to understand wind and solar based DG placement technique in better way.

### 3.1. Performance model of WTGU

Depending on the rotational speed WTGUs can be broadly categorized into two types namely fixed speed WTGU and variable speed WTGU. Fixed speed WTGU consists of direct grid coupled induction generator. In variable speed WTGU class, a wind turbine and an induction generator is connected with grid through back to back voltage source converter. Commonly variable speed WTGU is used in which real power output varies wind speed [28]. For a typical WTGU, the output electrical power generation is given by

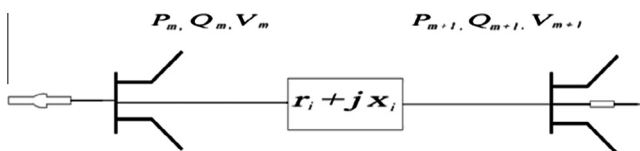


Fig. 1. Two bus section of radial distribution system.

$$P_w = \begin{cases} 0 & v_w < v_{cin} \text{ OR } v_w > v_{cout} \\ P_{rated} \frac{v_w^3 - v_{cin}^3}{v_N^3 - v_{cin}^3} & v_{cin} \leq v_w \leq v_N \\ P_{rated} & v_N \leq v_w \leq v_{cout} \end{cases} \quad (16)$$

$v_{cin}$ ,  $v_{cout}$ ,  $v_N$  are cut-in speed, cut-out speed and nominal speed of wind turbine, respectively;  $v_w$  is the average wind speed;  $P_{rated}$  is the rated output power of turbine and can be represented as

$$P_{rated} = 0.5 \rho A v_w^3 C_p \quad (17)$$

where  $A$  is the swept area of rotor;  $\rho$  is the density of air;  $v_w$  is wind speed and  $C_p$  is the power co-efficient.

### 3.2. Performance model of PV array

Solar radiation and ambient temperature are the main governors for sizing of PV module. PV module cannot generate bulk amount of electrical power. So, large number of PV modules are

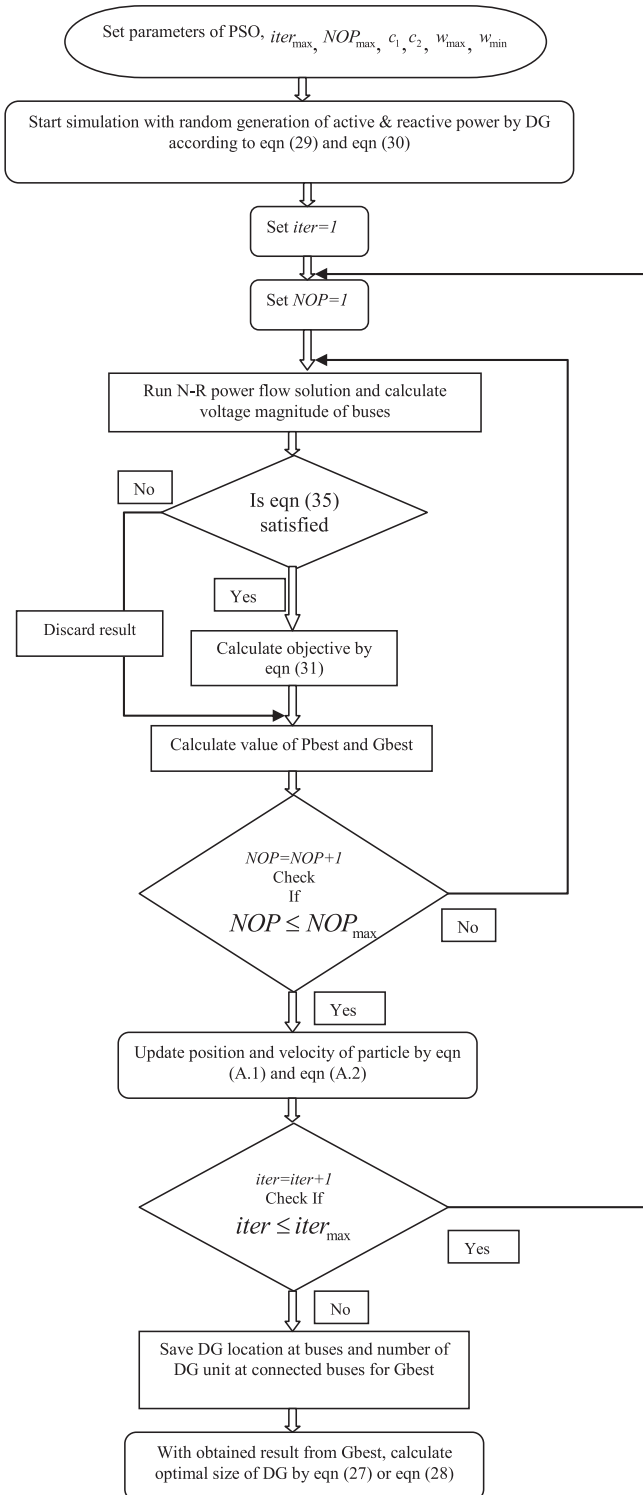


Fig. 2. Flowchart of PSO based DG placement technique.

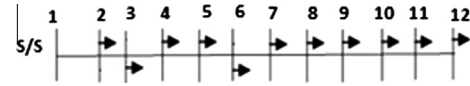


Fig. 3. Single Line Diagram (SLD) of 12-bus distribution system with Bus-1 connected to sub-station.

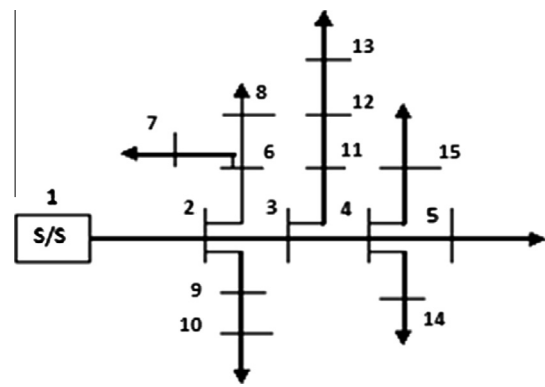


Fig. 4. SLD of 15-bus distribution system having Bus-1 as sub-station.

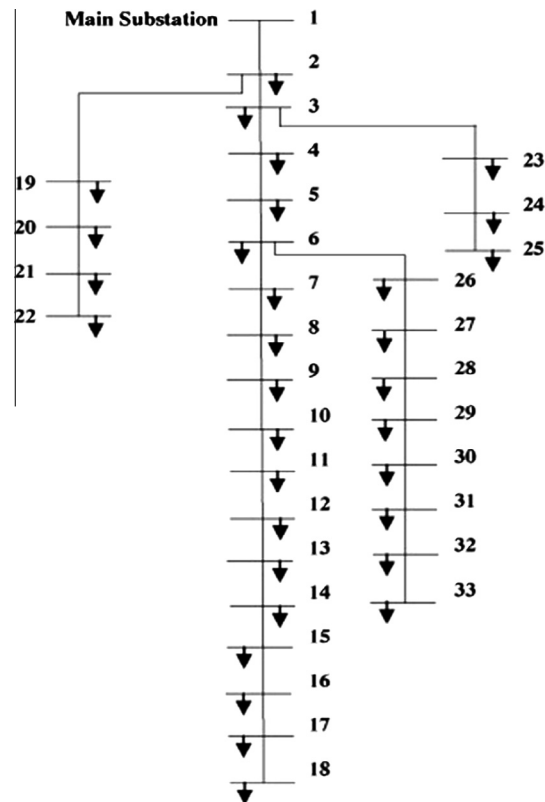


Fig. 5. SLD of 33-bus distribution system.

connected in series and parallel to design PV array. Series and parallel connection of PV modules boost up voltage and current to tailor PV array output. For a PV array consist of  $N_S \times N_P$  PV modules, maximum output power can be calculated as

$$P_{pv} = N_S N_P P_{md} \tag{18}$$

$P_{md}$  is the maximum electrical power generated by PV module which is formulated as

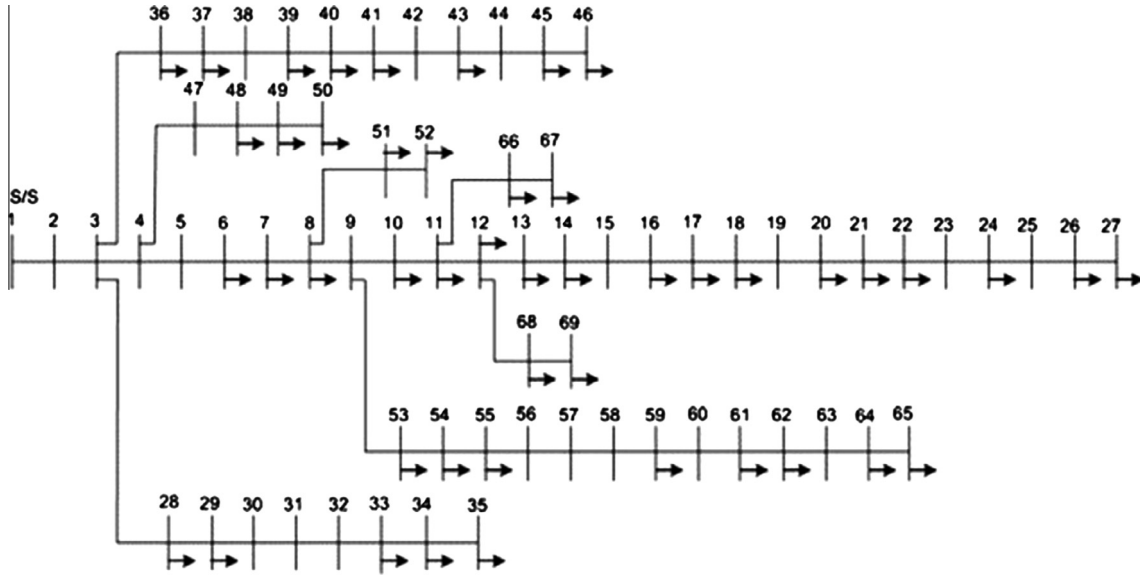


Fig. 6. SLD of 69-bus distribution system with Bus-1 as sub-station.

**Table 1**  
Determination of weak buses of different feeders for 12-bus, 15-bus, 33-bus and 69-bus test system by existing techniques and proposed VSF.

		Weak bus obtained by VSI [Jasmon]	Weak bus obtained by PSI [Aman]	Weak bus obtained by VSF
12-bus system	Feeder with Bus-2 ... 12	Bus-9	Bus-9	Bus-9
	Feeder with Bus-2 ... 5, 11 ... 15	Bus-11	Bus-11	Bus-11
15-bus system	Sub-feeder with Bus-6 ... 8	Bus-6	Bus-6	Bus-6
	Sub-feeder with Bus-9, 10	Bus-9	Bus-9	Bus-9
	Feeder with Bus-2 ... 18	Bus-17	Bus-17	Bus-17
33-bus system	Sub-feeder with Bus-19 ... 22	Bus-20	Bus-20	Bus-20
	Sub-feeder with Bus-23 ... 25	Bus-25	Bus-25	Bus-25
	Sub-feeder with Bus-26 ... 33	Bus-30	Bus-32	Bus-32
	Feeder with Bus-2 ... 27	Bus-26	Bus-26	Bus-26
69-bus system	Sub-feeder with Bus-28 ... 35	Bus-34	Bus-34	Bus-34
	Sub-feeder with Bus-36 ... 46	Bus-45	Bus-45	Bus-45
	Sub-feeder with Bus-47 ... 50	Bus-49	Bus-49	Bus-49
	Sub-feeder with Bus-51, 52	Bus-51	Bus-51	Bus-51
	Sub-feeder with Bus-53 ... 65	Bus-61	Bus-61	Bus-61
	Sub-feeder with Bus-66, 67	Bus-66	Bus-66	Bus-66
	Sub-feeder with Bus-68, 69	Bus-68	Bus-68	Bus-68

**Table 2**  
Verification of voltage stability variation with VSI and VSF method for different change of load levels in different systems (↓: improvement of voltage stability; ↑: decrement of voltage stability).

		VSI [Jasmon]	VSI [Shin]	VSF <sub>total</sub>
12-Bus system	At base load	0.1601	0.4582	10.4342
	With 60% increased load	0.2617 ↓	0.4297 ↓	10.0555 ↓
	With 30% reduced load	0.1123 ↑	0.4711 ↑	10.6115 ↑
15-Bus system	At base load	0.2050	0.4458	13.1538
	With 22% increased load	0.2503 ↓	0.4330 ↓	12.9530 ↓
	With 55% reduced load	0.0921 ↑	0.4764 ↑	13.6314 ↑
33-Bus system	At base load	0.3208	0.4122	28.9323
	With 41% increased load	0.4702 ↓	0.3639 ↓	27.3523 ↓
	With 14% reduced load	0.2720 ↑	0.4267 ↑	29.4160 ↑
69-Bus system	At base load	0.3163	0.4136	64.6850
	With 5% increased load	0.3345 ↓	0.4082 ↓	64.4902 ↓
	With 5% reduced load	0.2985 ↑	0.4189 ↑	64.8761 ↑

**Table 3**  
Parameters and their corresponding values of a Wind Turbine Generation Unit (WTGU).

Parameter of WTGU	Values
Rated output power, $P_{rated}$ (MW)	1
Cut-in-speed, $v_{cin}$ (m/s)	4
Nominal wind speed, $v_N$ (m/s)	16
Cut-out speed, $v_{cout}$ (m/s)	20

$$P_{md} = FF * V_{oc} * I_{sc} \tag{19}$$

$V_{oc}$ ,  $I_{sc}$  and FF are the open circuit voltage, short circuit current and fill factor of PV module.  $V_{oc}$ ,  $I_{sc}$  and FF are the function of solar irradiance and PV module temperature; and these are obtained as follows

$$V_{oc} = \frac{V_{Noc}}{1 + c_2 * \ln \left( \frac{G_N}{G_a} \right)^{c_1}} \tag{20}$$

$$I_{sc} = I_{Nsc} \left( \frac{G_a}{G_N} \right)^{c_3} \tag{21}$$

$$FF = \left( 1 - \frac{R_s}{V_{oc}/I_{sc}} \right) \frac{\frac{V_{oc}}{nKT/q} - \ln \left( \frac{V_{oc}}{nKT/q} + 0.72 \right)}{1 + \frac{V_{oc}}{nKT/q}} \tag{22}$$

**Table 4**  
Optimal location and number of WTGU units at unity power factor for 12-bus, 15-bus, 33-bus and 69-bus system along with voltage stability improvement and power loss reduction in each case.

	Number of connection bus	Location at bus (number of WTGU)	Value of $VSF_{total}$	Improvement of voltage stability (%)	Total power loss (kVA)	Power loss minimization (%)
12-Bus system	1	Bus-8 (2)	10.8534	4.0	14.7	4.67
15-Bus system	1	Bus-4 (5)	13.4558	2.30	62.1	38.15
	2	Bus-4 (4), Bus-7 (3)	13.5646	3.12	54.9	45.32
33-Bus system	1	Bus-12 (6)	30.9535	6.99	257.1	38.96
	2	Bus-12 (6), Bus-32 (5)	31.6698	9.46	171.9	59.18
	3	Bus-15 (6), Bus-24 (6), Bus-31 (4)	31.9204	10.33	152.3	63.84
	4	Bus-7 (5), Bus-16 (3), Bus-24 (5), Bus-30 (5)	31.9380	10.39	127.5	69.72
69-Bus system	1	Bus-61 (6)	65.7186	1.60	209.8	53.23
	2	Bus-62 (5), Bus-65 (4)	66.2075	2.35	171.2	61.84
	3	Bus-13 (6), Bus-59 (3), Bus-62 (5)	66.9482	3.49	152.8	65.94
	4	Bus-54 (5), Bus-59 (5), Bus-62 (3), Bus-65 (3)	66.8057	3.28	150.4	66.47
	5	Bus-7 (4), Bus-9 (2), Bus-48 (6), Bus-62 (6), Bus-64 (4)	67.1672	3.84	131.3	70.73

**Table 5**  
Comparative results of WTGU placement with power loss minimization based method; voltage stability based method and proposed technique at maximum penetration level DG with unity power factor.

		Power loss minimization based DG placement [10,12,15]	Voltage stability based DG placement [18]	Proposed method
12-Bus system	Location at bus (number of WTGU)	Bus-8 (2)	Bus-9 (1)	Bus-8 (2)
	$VSF_{total}$	10.8534	10.7001	10.8534
	Total power loss (kVA)	14.7	15.3	14.7
15-Bus system	Location at bus (number of WTGU)	Bus-4 (4), Bus-7 (3)	Bus-6 (6), Bus-11 (1)	Bus-3 (5), Bus-8 (2)
	$VSF_{total}$	13.4558	13.5312	13.5337
	Total power loss (kVA)	54.9	71.2	54.8
33-Bus system	Location at bus (number of WTGU)	Bus-7 (6), Bus-16 (4), Bus-24 (4), Bus-30 (4)	Bus-24 (6), Bus-25 (6), Bus-30 (4), Bus-32 (6)	Bus-7 (5), Bus-16 (3), Bus-24 (5), Bus-30 (5)
	$VSF_{total}$	31.1008	30.8079	31.9380
	Total power loss (kVA)	133.1	197	127.1
69-Bus system	Location at bus (number of WTGU)	Bus-7 (4), Bus-9 (2), Bus-48 (6), Bus-62 (6), Bus-64 (4)	Bus-49 (6), Bus-61 (6), Bus-64 (6), Bus-65 (1)	Bus-7 (4), Bus-9 (2), Bus-48 (6), Bus-62 (6), Bus-64 (4)
	$VSF_{total}$	66.706	66.7783	67.1672
	Total power loss (kVA)	143.7	160.7	131.3

$G_N$  and  $G_a$  are the nominal and actual solar irradiance on module;  $T_N$  and  $T_a$  are nominal and actual module temperature, respectively;  $V_{Noc}$  and  $I_{Nsc}$  are nominal the open circuit voltage and short circuit current of PV module;  $R_s$  is the series resistance of module;  $c_1$ ,  $c_2$  and  $c_3$  are the three different constant which are introduced to show non-linear relationship between solar irradiance, photo-current and cell temperature [29].  $n$  is density factor ( $n = 1.5$ );  $T$  is the PV module temperature (in Kelvin);  $K$  is Boltzman constant ( $1.38 \times 10^{-23}$  J/K); and  $q$  is the charge of electron ( $1.6 \times 10^{-19}$  C).

### 4. Optimal placement of DG

#### 4.1. DWA based multi objective PSO method

Particle swarm optimization is a powerful population based optimization strategy for finding maxima or minima in continuous nonlinear functions. Gbset PSO (referred to as PSO) utilizes stochastically velocity adjustment according to the historical best position for the particle itself and the neighborhood best position at each iteration [30]. The movement of each particle evolves to an optimal solution [Appendix A].

Many objectives are necessary to be handled simultaneously in multi objective optimization problem. In weighted aggregation multi objective PSO approach, all the objective functions are combined in a single one through a weighted combination [31].

$$F(x) = \sum_{i=1}^k wt_i \cdot f(x)_i \tag{23}$$

where  $wt_i$  are non-negative weights such that

$$\sum_{i=1}^k wt_i = 1 \tag{24}$$

And optimization is performed on  $F(x)$ , similarly to single objective case.

In DWA approach, the weights are changed gradually. The slow change of weights can be obtained by

$$wt(iter)_1 = |\sin(2\pi \cdot iter/Fr)| \tag{25}$$

$$wt(iter)_2 = 1 - wt(iter)_1 \tag{26}$$

where  $iter$  is the number of iteration and  $Fr$  is the adaptation frequency. The frequency should not be too high or too low so that the algorithm is able to converge to a minimum. It is reasonable to change the weight from 0 to 1 twice during the whole optimization [32].

#### 4.2. Location selection using multi objective PSO method

The importance of DGs in future smart grids increases considering the fact those DGs will have a role in system security, reliability, efficiency and quality as well. Considering that most DGs are located at the distribution level, determination of the best locations for installing DGs to maximize their benefits is very important in system design and expansion. In some literature sensitivity analysis based location selection is given. Some others have focused on DG placement on view point of power loss minimization. But, consideration of single objective always not gives optimal solution.

In this paper the DG placement issue is further examined.

Problem formulation:

The DG placement problem is formulated to meet multiple objective functions, including power loss minimization and voltage stability improvement. As the multiple DG units with same rating can be connected at P–Q buses, the number of DG units at different buses may not be equal. Total size of wind based DG for any Bus- $i$  can be calculated as

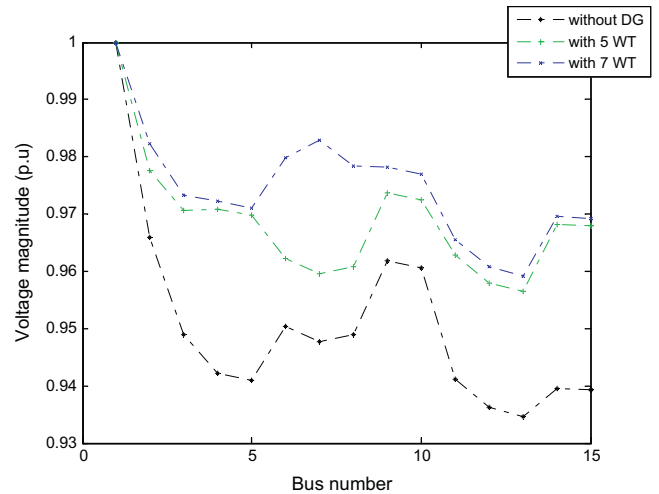


Fig. 8. Voltage magnitudes of 15-bus test system for different penetration scenarios WTGUs at unity p.f.

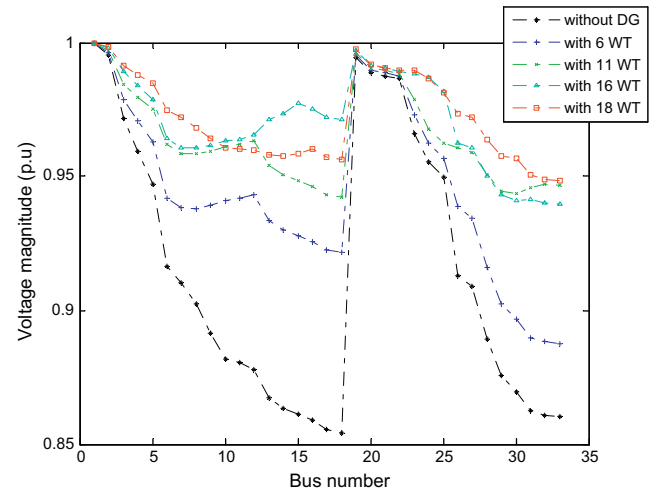


Fig. 9. Voltage magnitudes of 33-bus test system for different penetration scenarios WTGUs at unity p.f.

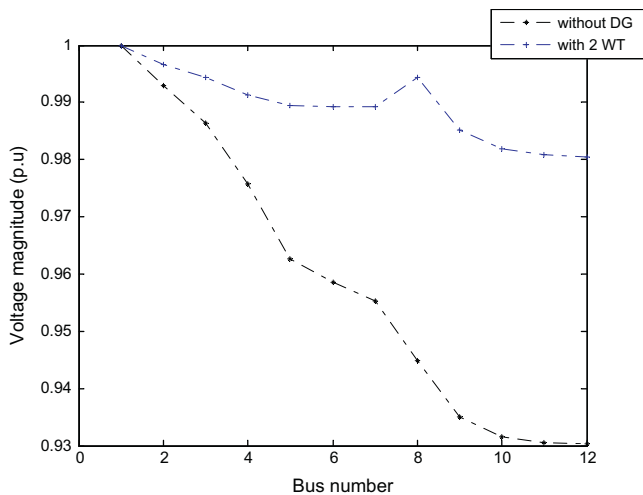


Fig. 7. Illustration of voltage magnitudes of 12-bus test system for different penetration scenarios of Wind Turbine Generation Unit (WTGU) at unity power factor (p.f.).

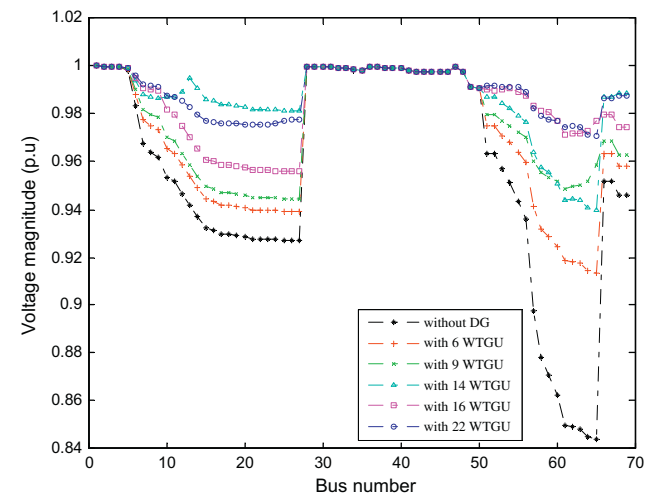
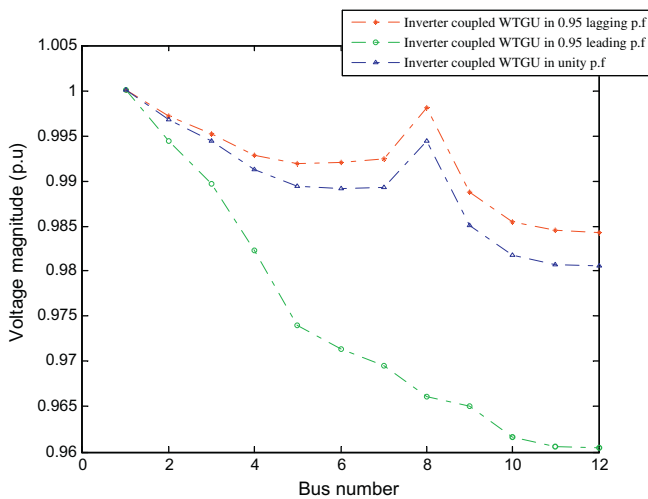


Fig. 10. Voltage magnitudes of 69-bus test system for different penetration scenarios WTGUs at unity p.f.

**Table 6**  
Comparative results of WTGU placement for 0.95 lagging and leading power factor (p.f) and unity power p.f mode at maximum penetration level DG.

		Location at bus (number of WTGU)	Total active power generation by DG (kW)	Total reactive power generation by DG (kVAR)	$VSF_{total}$	Total power loss (kVA)
12-Bus system	0.95 Lagging p.f	Bus-8 (2)	319	105	10.886	7.9
	Unity p.f	Bus-8 (2)	336	0	10.8534	14.7
	0.95 Leading p.f	Bus-8 (1)	160	-52	10.6556	82
15-Bus system	0.95 Lagging p.f	Bus-4 (4), Bus-7 (3)	1117	367	13.6672	29.9
	Unity p.f	Bus-3 (5), Bus-8 (2)	1176	13.5856	13.5337	54.8
	0.95 Leading p.f	Bus-7 (2), Bus-15 (2)	638.4	-199	13.3189	82
33-Bus system	0.95 Lagging p.f	Bus-11 (5), Bus-25 (4), Bus-29 (5), Bus-32 (4)	2873	943	31.515	55.8
	Unity p.f	Bus-7 (5), Bus-16 (3), Bus-24 (5), Bus-30 (5)	3024	31.938	127.1	
	0.95 leading p.f	Bus-5 (4), Bus-15 (4), Bus-25 (5), Bus-31 (4)	2713	-847	30.339	257.8
69-Bus system	0.95 Lagging p.f	Bus-7 (3), Bus-9 (3), Bus-48 (6), Bus-62 (6), Bus-64 (5)	3670	1205	67.0937	62.1
	Unity p.f	Bus-7 (4), Bus-9 (2), Bus-48 (6), Bus-62 (6), Bus-64 (4)	3696	0	67.1672	131.3
	0.95 Leading p.f	Bus-8 (3), Bus-29 (5), Bus-59 (4), Bus-61 (3), Bus-66 (3)	2873	-896	66.0065	266.9



**Fig. 11.** Voltage magnitudes of 12-bus system for optimal placement of WTGUs in 0.95 lagging, leading and unity p.f mode.

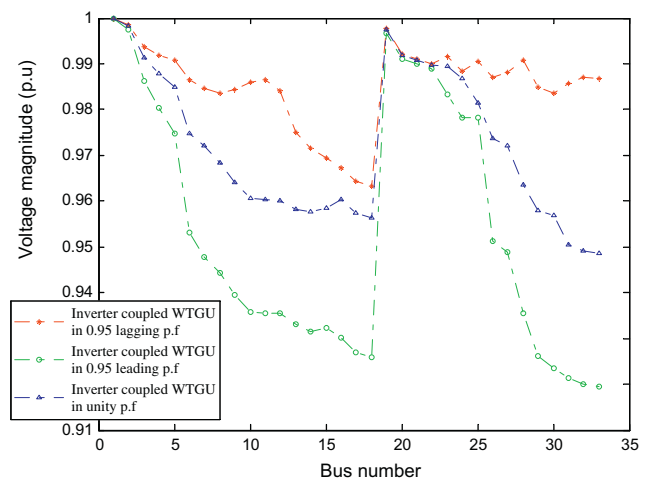


**Fig. 13.** Voltage magnitudes of 33-bus system for optimal placement of WTGUs in 0.95 lagging, leading and unity p.f mode.

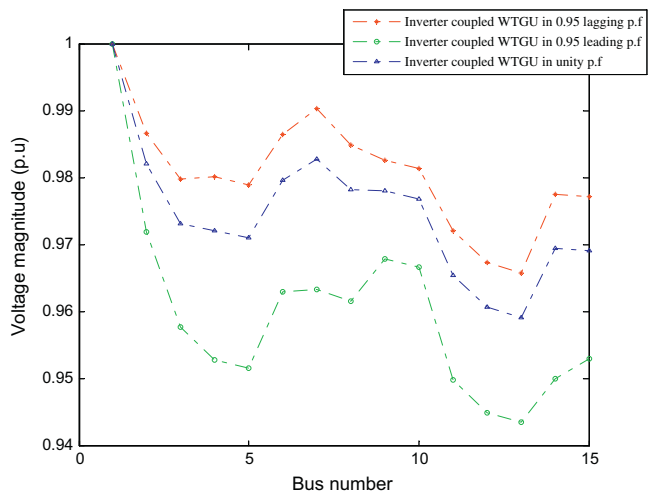


**Fig. 12.** Voltage magnitudes of 15-bus system for optimal placement of WTGUs in 0.95 lagging, leading and unity p.f mode.

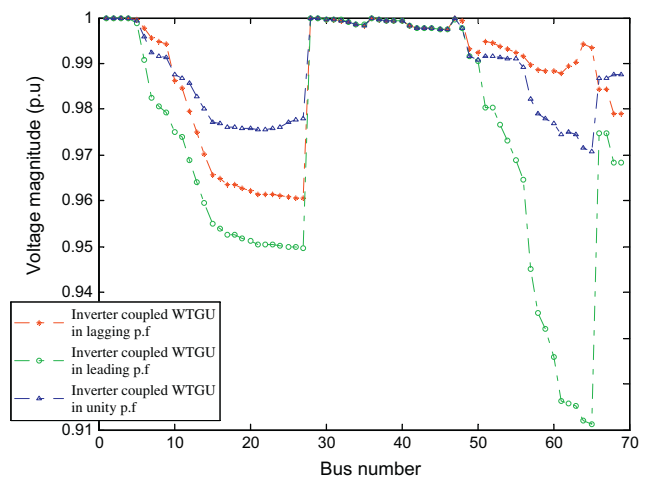


**Fig. 14.** Voltage magnitudes of 69-bus system for optimal placement of WTGUs in 0.95 lagging, leading and unity p.f mode.

$$DG_{wind,i} = \sum_{n_i=1}^{n_{i,max}} n_i * P_w \tag{27}$$

In case of installation of PV array total power generation at any Bus-*i* can be determined as

$$DG_{pv,i} = \sum_{n_i=1}^{n_{i,max}} n_i * P_{pv} \tag{28}$$

where *n<sub>i</sub>* is number of DG unit that can be connected at Bus-*i* and varied within range {1, *n<sub>i,max</sub>*}. *n<sub>i,max</sub>* is the maximum number of DG unit for any Bus-*i*.

**Table 7**  
Parameters and their corresponding values of a PV module.

PV module parameter	Values
Maximum output, <i>P<sub>max</sub></i> (W)	100
Nominal solar intensity on module, <i>G<sub>N</sub></i> (W/m <sup>2</sup> )	1000
Nominal open circuit voltage at <i>V<sub>Noc</sub></i> (V)	21
Nominal short circuit current at <i>I<sub>Nsc</sub></i> (A)	6.5
Series resistance, <i>R<sub>se</sub></i> (ohm)	0.012
Nominal cell operating temperature, <i>T<sub>N</sub></i> (°C)	25

**Table 8**  
Optimal location and number of installed PV arrays at unity power factor mode for 12-bus, 15-bus, 33-bus and 69-bus system along with voltage stability improvement and power loss reduction in each step.

	Number of connection bus	Location at bus (number of PV array)	Value of <i>V<sub>SF</sub><sub>total</sub></i>	Improvement of voltage stability (%)	Total power loss (kVA)	Power loss minimization (%)
12-bus system	1	Bus-9 (5)	10.8429	3.92	14.3	4.82
	2	Bus-5 (4), Bus-10 (3)	10.8698	4.17	12.5	5.47
15-bus system	1	Bus-15 (5)	13.2586	0.8	80.2	20.12
	2	Bus-4 (5), bus-15 (5)	13.3536	1.51	67.6	32.67
	3	Bus-4 (4), Bus-7 (5), Bus-12 (3)	13.3976	1.85	60.8	39.44
	4	Bus-6 (4), Bus-11 (5), Bus-13 (3), Bus-15 (4)	13.4877	2.54	55.1	45.12
	5	Bus-2 (5), Bus-5 (5), Bus-6 (3), Bus-7 (4), Bus-11 (5)	13.5378	2.92	51.8	48.41
	6	Bus-5 (4), Bus-6 (4), Bus-8 (5), Bus-9 (3), Bus-12 (4), Bus-15 (4)	13.6146	3.50	51.4	48.80
33-bus system	1	Bus-16 (6)	29.3693	1.51	337.4	19.89
	2	Bus-15 (6), Bus-31 (6)	29.6534	2.49	271.0	35.66
	3	Bus-8 (6), Bus-18 (6), Bus-29 (5)	29.8432	3.15	245.7	41.66
	4	Bus-8 (6), Bus-10 (5), Bus-18 (6), Bus-29 (6)	30.1385	4.17	209.5	50.26
	5	Bus-11 (6), Bus-13 (6), Bus-16 (5), Bus-26 (5), Bus-33 (6)	30.4258	5.16	185.6	55.93
	6	Bus-10 (5), Bus-12 (6), Bus-17 (5), Bus-23 (5), Bus-29 (6), Bus-30 (6)	30.4664	5.30	170.6	59.49
	7	Bus-8 (5), Bus-9 (4), Bus-12 (4), Bus-17 (6), Bus-26 (6), Bus-29 (6), Bus-33 (4)	30.6017	5.77	159.8	62.06
	8	Bus-10 (5), Bus-8 (5), Bus-17 (5), Bus-24 (5), Bus-26 (4), Bus-30 (5), Bus-31 (5), Bus-33 (5)	30.6441	5.92	148.4	64.76
	9	Bus-7 (3), Bus-10 (3), Bus-15 (6), Bus-18 (6), Bus-24 (5), Bus-26 (6), Bus-27 (4), Bus-31 (6), Bus-33 (4)	30.9501	6.97	141.6	66.38
	10	Bus-8 (6), Bus-13 (6), Bus-16 (3), Bus-17 (6), Bus-20 (6), Bus-24 (6), Bus-25 (6), Bus-27 (6), Bus-31 (6), Bus-33 (6)	31.0781	7.42	127.0	69.84
	11	Bus-65 (6)	65.0513	0.6	347.9	22.45
2	Bus-59 (5), Bus-65 (6)	65.2984	1.0	292.5	34.79	
3	Bus-59 (4), Bus-61 (6), Bus-65 (6)	65.5670	1.36	238.1	46.92	
4	Bus-24 (6), Bus-64 (6), Bus-65 (5), Bus-68 (3)	65.8554	1.81	246.2	45.12	
5	Bus-8 (5), Bus-9 (1), Bus-24 (5), Bus-59 (6), Bus-62 (6)	65.9396	1.94	244.2	45.56	
6	Bus-54 (2), Bus-59 (2), Bus-61 (4), Bus-62 (6), Bus-65 (6), Bus-69 (6)	65.9890	2.02	195.1	56.51	
7	Bus-8 (4), Bus-12 (4), Bus-59 (4), Bus-61 (5), Bus-62 (6), Bus-65 (4), Bus-68 (5)	66.1126	2.21	180.7	59.71	
8	Bus-7 (3), Bus-54 (2), Bus-59 (2), Bus-61 (4), Bus-62 (6), Bus-65 (6), Bus-67 (4), Bus-69 (6)	66.1808	2.31	176.4	58.45	
9	Bus-8 (2), Bus-16 (2), Bus-49 (3), Bus-51 (4), Bus-54 (4), Bus-61 (6), Bus-65 (5), Bus-68 (6), Bus-69 (5)	66.2230	2.38	208.7	53.48	
10	Bus-20 (4), Bus-27 (5), Bus-29 (1), Bus-37 (6), Bus-43 (3), Bus-62 (6), Bus-64 (6), Bus-65 (3), Bus-66 (2), Bus-68 (3)	66.4024	2.66	206.2	54.04	
11	Bus-6 (3), Bus-8 (5), Bus-12 (5), Bus-26 (6), Bus-52 (5), Bus-53 (6), Bus-59 (5), Bus-61 (6), Bus-62 (6), Bus-65 (5), Bus-68 (6)	67.1558	3.82	148.6	66.87	

Generally DGs are operated at unity power factor (p.f) to supply only active power. However with recent technological advancement has created the opportunity to operate coupled inverter between solar or wind generation unit and Point of Common Coupling (PCC) at other p.f mode also. As a result the inverters can supply both active and reactive power. If *cos θ* is the p.f at PCC, the active and reactive power output of coupled inverter based WTGU or PV array can be given by

$$P_{DG,i} = I_i * DG_i * \cos \theta \tag{29}$$

$$Q_{DG,i} = I_i * DG_i * (\sqrt{1 - \cos^2 \theta}) \tag{30}$$

*DG<sub>i</sub>* would become *DG<sub>wind,i</sub>* in placement planning of wind based DG and *DG<sub>pv,i</sub>* in case of solar based DG installation. *I<sub>i</sub>* is the location variable at Bus-*i* which may be one or zero depending on connection or not connection of DG.

*Sloss<sub>total</sub>* and *VSF<sub>total</sub>* are the function of *P<sub>DG,i</sub>* (*Sloss<sub>total</sub>*, *VSF<sub>total</sub>* = *f*(*P<sub>DG,i</sub>*, *Q<sub>DG,i</sub>*)) which are determined through power flow solution. *Sloss<sub>total</sub>* is the total power loss of the network.

In current study, problem is to find optimal location of DG in the network for varying number of DG units to get optimal solution of objective function. The overall objective function, with composing constraints and goals, is determined as follows.

**Table 9**  
Results from different PV array placement technique namely power loss minimization based method; voltage stability based placement method; and technique aiming minimization of power loss and maximization of voltage stability at maximum penetration level DG with unity power factor.

		Power loss minimization based DG placement [10,12,15]	Voltage stability based DG placement [18]	Proposed method
12-Bus system	Location at bus (number of PV array)	Bus-6 (3), Bus-10 (3)	Bus-9 (5)	Bus-5 (4), Bus-10 (3)
	$VSF_{total}$	10.8433	10.8429	10.8698
	Total power loss (kVA)	12.4	14.3	12.5
15-Bus system	Location at bus (number of PV array)	Bus-4 (5), Bus-6 (3), Bus-8 (4), Bus-9 (4), Bus-12 (6), Bus-14 (2)	Bus-6 (6), Bus-7 (6), Bus-8 (6), Bus-11 (6)	Bus-5 (4), Bus-6 (4), Bus-8 (5), Bus-9 (3), Bus-12 (4), Bus-15 (4)
	$VSF_{total}$	13.6117	13.5856	13.6146
	Total power loss (kVA)	50.9	67.0	50.9
33-Bus system	Location at bus (number of PV array)	Bus-7 (5), Bus-9 (6), Bus-12 (5), Bus-18 (6), Bus-19 (6), Bus-24 (6), Bus-27 (5), Bus-28 (6), Bus-29 (6), Bus-32 (6)	Bus-24 (6), Bus-25 (6), Bus-30 (6), Bus-32 (4)	Bus-8 (6), Bus-13 (6), Bus-16 (3), Bus-17 (6), Bus-20 (6), Bus-24 (6), Bus-25 (6), Bus-27 (6), Bus-31 (6), Bus-33 (6)
	$VSF_{total}$	31.0706	29.5745	31.0781
	Total power loss (kVA)	131.5	266.5	127.0
69-Bus system	Location at bus (number of PV array)	Bus-6 (4), Bus-8 (5), Bus-13 (6), Bus-17 (4), Bus-36 (4), Bus-46 (3), Bus-48 (6), Bus-51 (6), Bus-59 (4), Bus-64 (2), Bus-65 (6)	Bus-12 (6), Bus-48 (6), Bus-49 (6), Bus-50 (6), Bus-59 (6), Bus-61 (6), Bus-64 (6), Bus-65 (6)	Bus-6 (3), Bus-8 (5), Bus-12 (5), Bus-26 (6), Bus-52 (5), Bus-53 (6), Bus-59 (5), Bus-61 (6), Bus-62 (6), Bus-65 (5), Bus-68 (6)
	$VSF_{total}$	66.227	66.24	67.1558
	Total power loss (kVA)	217.2	164.2	148.6

Objective function is composed of power loss function which would be minimized and VSF function which would be maximized (i.e.  $(1/VSF_{total})$  would be minimized).

Objective:

$$f(Sloss_{total}, VSF_{total}) = \{wt(ite r)_1 \cdot Sloss_{total} + wt(ite r)_2 \cdot (1/VSF_{total})\} \tag{31}$$

$Sloss_{total}$  for 'n' number of branches in the system and can be calculated as

$$Sloss_{total} = \sum_{i=1}^n \sqrt{(Ploss_i^2 + Qloss_i^2)} \tag{32}$$

Power flow constraint:

$$P_{G,i} + P_{DG,i} - P_{D,i} = \sum_{j=1}^n V_i^2 \cdot Y_{ij}^2 \cdot \cos(\theta_{ij} + \lambda_j - \lambda_i); \quad i \in \{1, 2, \dots, n\} \tag{33}$$

$$Q_{G,i} + Q_{DG,i} - Q_{D,i} = \sum_{j=1}^n V_i^2 \cdot Y_{ij}^2 \cdot \sin(\theta_{ij} + \lambda_j - \lambda_i); \quad i \in \{1, 2, \dots, n\} \tag{34}$$

Voltage constraint:

$$|V_{i,bus}| \leq 1.05 \text{ p.u} \tag{35}$$

The flow chart of the methodology has been presented in flow chart at Fig. 2.

**5. Simulation results and discussion**

*5.1. Validation of VSF*

12-Bus, 15-bus, 33-bus and 69-bus radial distribution systems are simulated in MATLAB environment to validate proposed VSF.

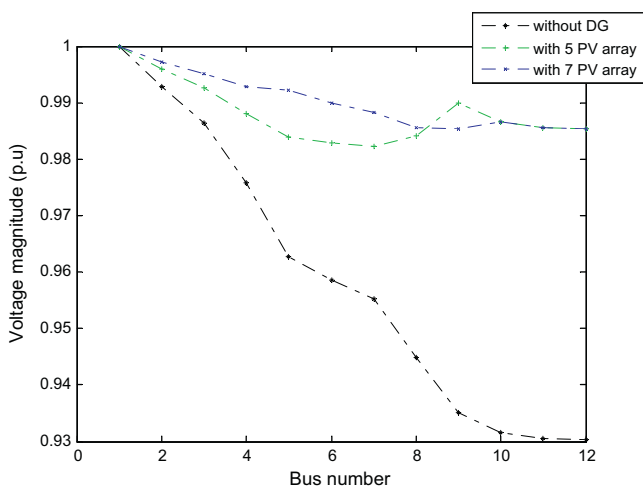


**Fig. 15.** Variation of voltage magnitudes of 12-bus test system for different penetration scenarios of PV arrays.

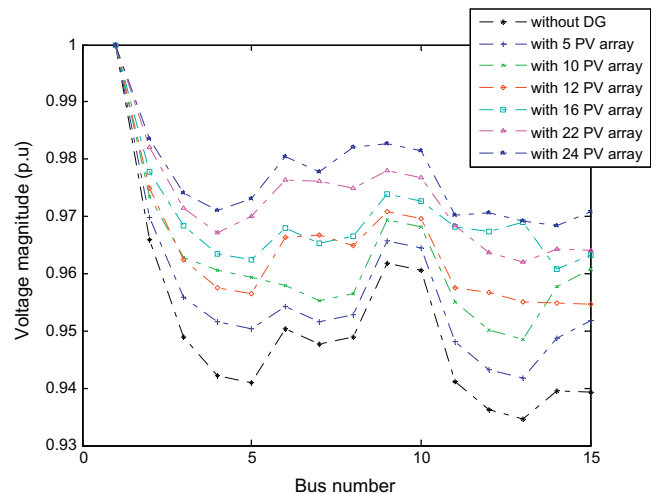


**Fig. 16.** Voltage magnitudes of 15-bus test system for different penetration scenarios PV arrays.

Newton–Raphson algorithm based power flow program is used to solve the power flow problem.

Single line diagram of 12-bus, 15-bus, 33-bus and 69-bus systems are shown in Figs. 3–6, respectively. The 12-bus test system is a radial feeder with 11 branches and total load of  $435 + j405$  kVA [33]. The 15-bus rural distribution system have total load of  $1.226 + j1.251$  MVA [34]. The 33-bus distribution system is radial in nature with 32 branches having total load of  $3.715 + j2.3$  MVA [35]. 69-bus distribution system has total load of  $3.803 + j2.693$  MVA. Line and load data of 69 bus radial network is given in [36].

Complex voltages of all the load buses are calculated using power flow solution technique. VSI by Jasmon, PSI and VSF are calculated for load buses of different test system utilizing given system data and obtained bus voltage. Weak buses identified in all the main feeders and sub-feeders of different test systems and tabulated in Table 1. It is verified that proposed VSF can identify the weak buses correctly. VSF is also helpful to measure total voltage stability level of the system. System loads are randomly increased and decreased to show the variation of voltage stability level. Obtained results are verified with VSI by Jasmon and VSI by Shin. Voltage stability levels of the networks decrease for increased load and voltage stability increase for reduction of load as shown in Table 2. In comparison with other VSI and PSI, less data are required for VSF to measure voltage stability as it is calculated only in voltage dimension. In conjunction with voltage, other system data such as load data and line data are also required in case of other index. As a result other stability index needs more complex calculation than VSF.

### 5.2. Results of DG placement

DG placement technique has been tested on 12-bus, 15-bus, 33-bus and 69-bus distribution system. Simulations are carried out on Intel (R) Core (TM) 2 Duo processor with 2.0 GB RAM using MATLAB 7.10.

Without DG, minimum value of voltage magnitude is obtained as 0.9303 p.u at Bus-12 for 12-bus system, 0.9306 p.u at Bus-15 for 15-bus system, 0.854 p.u at Bus-18 for 33-bus system and 0.8441 p.u at Bus-65 for 69-bus system. The 12-bus, 15-bus, 33-bus and 69-bus test systems incur total power loss of 27.6 kVA, 100.4 kVA, 421 kVA and 448.6 kVA, respectively. Values of VSF for 12-bus, 15-bus, 33-bus and 69-bus test systems are calculated as 10.4342, 13.1538, 28.9323 and 64.6851, respectively. So, there is

provision of improvement of voltage stability level and reduction of power loss for test systems using DG on the aspect of supply better quality power at the consumer end.

IEEE 1547 standard have recommended that DG should operate with unity power factor or fixed p.f near to unity with respect to the local system. Most of the distribution authorities and independent power producers have considered maximum  $\pm 0.95$  p.f operation mode of DG [37].

Maximum Number of Particles ( $NOP_{max}$ ) and maximum iteration ( $iter_{max}$ ) are set 200 and 500 respectively in PSO algorithm for 12-bus and 15-bus test systems. As number of variables increases with increase size of test system,  $NOP_{max}$  is chosen 500 for 33-bus and 69-bus test system. Adaptation frequency is set at 1000 to evaluate  $\min \{f(Sloss_{total}, VSF_{total})\}$  for test systems. The results obtained by PSO are verified by Inertia Adaptive PSO (IAPSO) and Fully Informed PSO (FIPSO). Values of adaptation frequency,  $NOP_{max}$  and  $iter_{max}$  in IAPSO [38] and FIPSO [39] are set same as used in PSO. It is considered that maximum six DG unit can be connected in parallel at any bus.

#### 5.2.1. Case 1: WTGU placement

Before placement, size of WTGU is calculated by (16). Average wind speed of Srinagar, north Indian region with latitude of 34.08366 and longitude of 74.79737 is incorporated in the study [40]. Required parameters of WTGU [41] are given in Table 3. With annual average wind speed 6.02 m/s in the year of 2012, power generation of WTGU is calculated 168 kW.

Utilities may be interested to locate WTGU at certain number of buses. Considering the fact, detail allocation of WTGU from minimum penetration to maximum is experimented. Results of WTGU placement at unity p.f mode of inverters for 12-bus, 15-bus, 33-bus and 69-bus systems obtained from PSO are tabulated in Table 4. The results executed by PSO agree with results from IAPSO and FIPSO. Results in Table 4 shows the optimal WTGU locations in the network along with optimum number of units that can be connected at buses. As the penetration of WTGU increases, VSF approaches towards one which suggests that voltage stability condition of the system is improving. The power losses are reduced as penetration of WTGU increases. At highest penetration point of wind based DG, voltage stability level of 4%, 3.12%, 10.39% and 3.84% can be maximized and 4.67%, 45.32%, 69.72% and 70.73% power losses can be minimized for 12-bus, 15-bus, 33-bus and 69-bus test system, respectively.

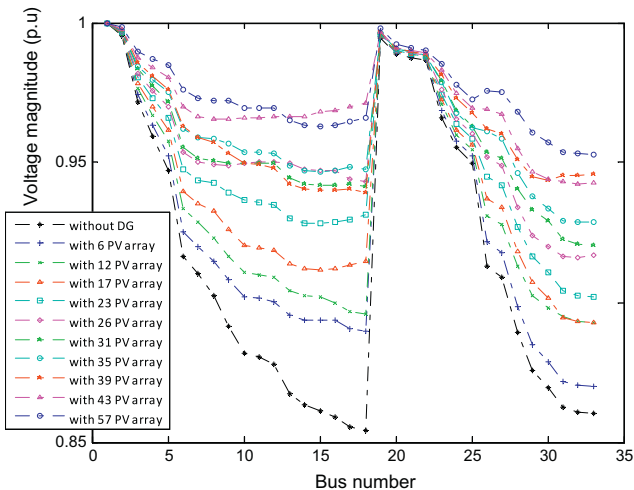


Fig. 17. Voltage magnitudes of 33-bus test system for different penetration scenarios PV arrays.

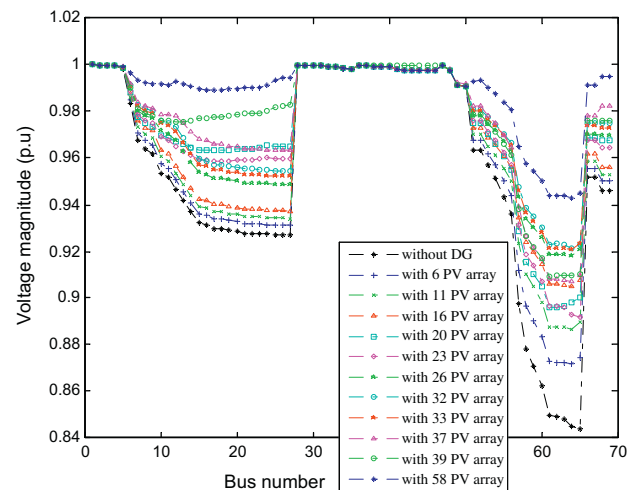


Fig. 18. Voltage magnitudes of 69-bus test system for different penetration scenarios PV arrays.

**Table 10**

Comparative study of voltage stability and total power losses along with optimal location of PV arrays in 12-bus, 15-bus, 33-bus and 69-bus distribution system at different power factor (p.f) mode.

		Location at bus (number of PV array)	Total active power generation by DG (kW)	Total reactive power generation by DG (kVAR)	VSF <sub>total</sub>	Total power loss (kVA)
12-Bus system	0.95 Lagging p.f	Bus-5 (4), Bus-10 (3)	351	115	10.9	5.6
	Unity p.f	Bus-5 (4), Bus-10 (3)	370	0	10.8698	12.5
	0.95 Leading p.f	Bus-7 (2), Bus-9 (2)	201	-63	10.6597	20
15-Bus system	0.95 Lagging p.f	Bus-5 (4), Bus-6 (4), Bus-8 (5), Bus-12 (5), Bus-14 (1), Bus-15 (5)	1154	379	13.728	25.1
	Unity p.f	Bus-5 (4), Bus-6 (4), Bus-8 (5), Bus-9 (3), Bus-12 (4), Bus-15 (4)	1267	0	13.6146	50.9
	0.95 Leading p.f	Bus-6 (4), Bus-7 (1), Bus-9 (2), Bus-11 (1), Bus-13 (2), Bus-14 (3)	652	-204	13.326	79.7
33-Bus system	0.95 Lagging p.f	Bus-12 (6), Bus-14 (6), Bus-16 (4), Bus-20 (2), Bus-23 (6), Bus-27 (2), Bus-29 (6), Bus-30 (6), Bus-32 (6), Bus-33 (5)	2458	807	31.3933	63.5
	Unity p.f	Bus-8 (6), Bus-13 (6), Bus-16 (3), Bus-17 (6), Bus-20 (6), Bus-24 (6), Bus-25 (6), Bus-27 (6), Bus-31 (6), Bus-33 (6)	2693	0	31.0781	127.0
	0.95 Leading p.f	Bus-2 (2), Bus-5 (4), Bus-6 (2), Bus-14 (1), Bus-18 (5), Bus-21 (3), Bus-23 (4), Bus-25 (6), Bus-28 (6), Bus-33 (6)	1956	-642	29.8828	257.0
69-Bus system	0.95 Lagging p.f	Bus-7 (5), Bus-16 (4), Bus-51 (3), Bus-54 (5), Bus-59 (4), Bus-61 (5), Bus-62 (6), Bus-65 (4), Bus-67 (5), Bus-68 (5), Bus-69 (6)	2608	857	67.1103	96.8
	Unity p.f	Bus-6 (3), Bus-8 (5), Bus-12 (5), Bus-26 (6), Bus-52 (5), Bus-53 (6), Bus-59 (5), Bus-61 (6), Bus-62 (6), Bus-65 (5), Bus-68 (6)	3062	0	67.1558	148.6
	0.95 Leading p.f	Bus-8 (4), Bus-18 (4), Bus-51 (1), Bus-53 (3), Bus-59 (3), Bus-61 (5), Bus-62 (6), Bus-65 (3), Bus-66 (3), Bus-68 (6), Bus-69 (4)	2108	-658	66.2248	269.0

The proposed methodology is compared with other DG placement technique in Table 5. VSI based DG placement method is not suitable for multiple DG placement. The result obtained on the basis of power loss minimization technique is quite competent and results match with proposed methodology in some cases. But, data of Table 5 reflect that proposed method can allocate WTGU in better way to improve voltage stability of the network and reduce system power losses.

Most of the bus voltage magnitudes are increased significantly after installation of WTGUs at unity p.f mode as shown in Figs. 7–

10, respectively for 12-bus, 15-bus, 33-bus and 69-bus system. Minimum bus voltage of the system has boosted up highly for maximum penetration of WTGU. Minimum bus voltage magnitude 0.9805 p.u at Bus-12, 0.9592 p.u at Bus-13, 0.9523 p.u at Bus-33 and 0.9707 p.u at Bus-65 are generated for 12-bus, 15-bus, 33-bus and 69-bus, respectively at maximum penetration of wind based DG.

WTGUs deployment for 0.95 lagging and leading p.f mode of converters are also simulated with proposed methodology and obtained results are compared with unity p.f mode of inverters at

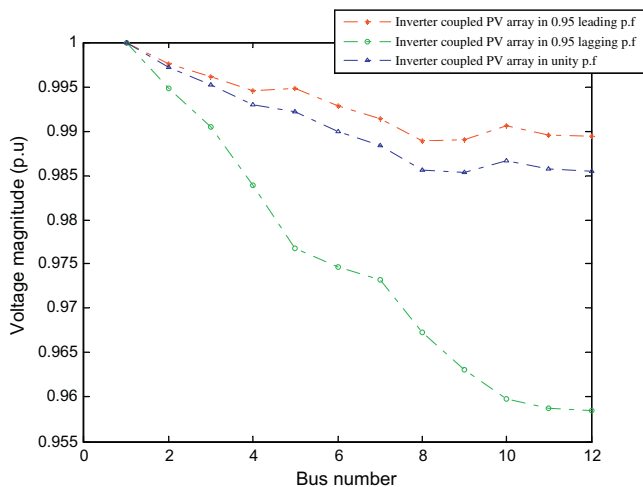


**Fig. 19.** Graphical comparison of voltage magnitudes for optimal placement of PV arrays for 0.95 lagging, leading and unity p.f mode in case of 12-bus system.

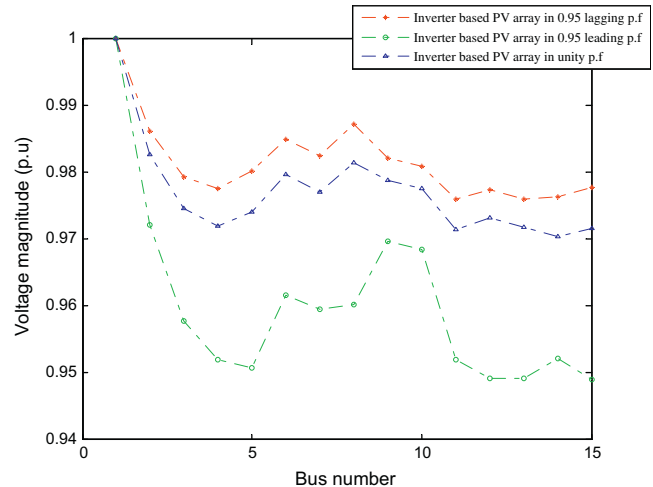


**Fig. 20.** Graphical comparison of voltage magnitudes for optimal placement of PV arrays for 0.95 lagging, leading and unity p.f mode in case of 15-bus system.

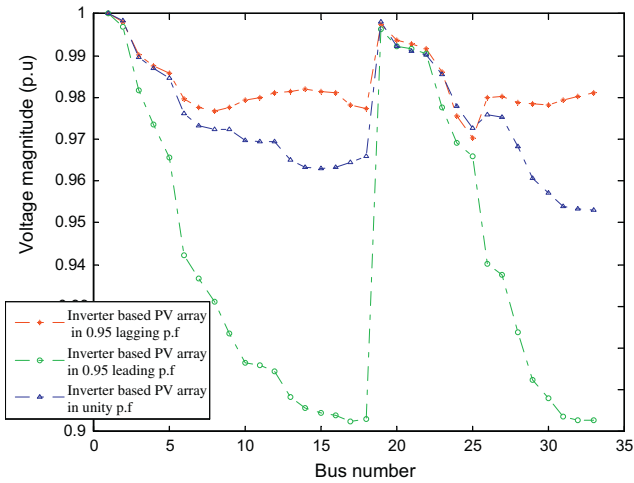


**Fig. 21.** Graphical comparison of voltage magnitudes for optimal placement of PV arrays for 0.95 lagging, leading and unity p.f mode in case of 33-bus system.

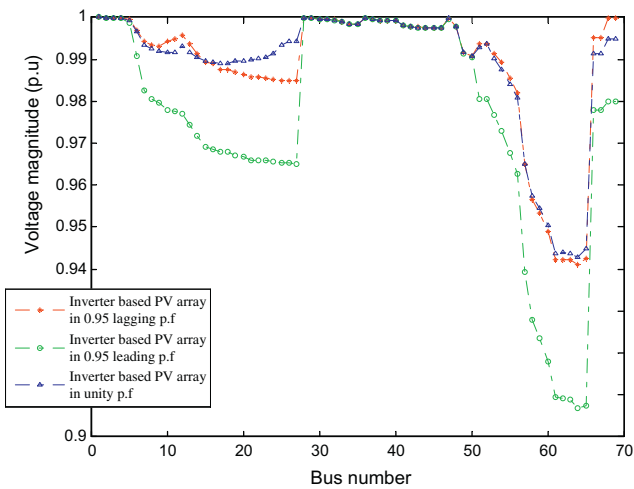


**Fig. 22.** Graphical comparison of voltage magnitudes for optimal placement of PV arrays for 0.95 lagging, leading and unity p.f mode in case of 69-bus system.

maximum penetration level in Table 6. Size and location of WTGU has been changed for consideration of different p.f mode and results are given in Table 6. The results show that reactive power supply capability of inverter based WTGU at 0.95 lagging p.f mode can be helpful for significant power loss reduction and voltage stability improvement. Maximum rise of voltage magnitudes at most of the buses through reactive power supply of WTGU for 12-bus, 15-bus, 33-bus and 69-bus are shown in Figs. 11–14, respectively. On the other hand, active power feeding and reactive power absorption characteristics of inverter based DGs at 0.95 leading p.f mode causes lower voltage profile rise.

**5.2.2. Case 2: PV array placement**

To calculate output power of PV array by (18), average solar irradiance and cell temperature data are needed. With annual solar irradiation average of 192.917 W/m<sup>2</sup> in the year of 2012 at Srinagar [42] and cell temperature of 15 °C, maximum output power of PV array is determined as 52.8 kW. Required parameters of PV module [43] are given in Table 7.

Detail results with step by step allocation of PV array up to maximum penetration for different test systems for unity p.f operation of inverters are presented in Table 8. Results illustrate the number of PV array that can be connected at optimal bus location for diverse penetration scenario. At maximum penetration level of PV array, voltage stability levels of systems are enhanced by 4.17%, 3.50%, 7.42% and 3.82% for 12-bus, 15-bus, 33-bus and 69-bus test systems. Total network losses are reduced by 5.47%, 48.80%, 69.84% and 66.87% for 12-bus, 15-bus, 33-bus and 69-bus respectively at the point maximum PV array connection.

Proposed methodology is compared with some other existing techniques. From Table 9, it is clarified that proposed method can generate very promising results in the context of multiple PV array placements. It can cause maximum reduction of power loss and improvement of voltage stability with proper number of PV arrays at optimal bus locations.

Improvement of voltage magnitudes via installation of inverter based PV arrays at unity p.f mode is shown in Figs. 15–18 for test systems. In case of maximum penetration of solar based DG, minimum voltages become 0.9823 p.u at Bus-9, 0.9705 p.u at Bus-14, 0.9483 p.u at Bus-33 and 0.95 p.u at Bus-64 for 12-bus, 15-bus, 33-bus and 69-bus, respectively.

**Table 11**  
Comparative study simulation time of FIPSO, IAPSO and PSO at maximum penetration level of WTGU at unity p.f mode for different test systems.

	FIPSO		IAPSO		PSO	
	Simulation time (s)	Average simulation time (s)	Simulation time (s)	Average simulation time (s)	Simulation time (s)	Average simulation time (s)
12-Bus system	126.12	126.586	127.17	128.976	124.89	122.428
	125.54		129.14		122.34	
	127.52		128.78		121.25	
	127.25		129.36		121.54	
	126.50		130.43		122.12	
15-Bus system	155.40	156.390	165.08	166.242	150.94	151.560
	155.71		165.96		151.97	
	157.08		166.21		152.22	
	156.55		165.92		151.37	
	157.21		168.04		151.30	
33-Bus system	1091.45	1096.278	1152.67	1141.578	1068.22	1075.064
	1108.40		1148.76		1070.25	
	1090.76		1138.31		1102.07	
	1094.57		1127.52		1067.42	
	1096.21		1141.53		1067.36	
69-Bus system	6285.18	6189.71	7032.72	7079.76	6047.96	6059.37
	6159.45		7137.64		6069.18	
	6134.11		7074.66		6069.50	
	6188.57		7069.45		6057.38	
	6181.26		7084.35		6052.84	

**Table 12**  
Comparative study simulation time of FIPSO, IAPSO and PSO at maximum penetration level of PV array at unity p.f mode for different test systems.

	FIPSO		IAPSO		PSO	
	Simulation time (s)	Average simulation time (s)	Simulation time (s)	Average simulation time (s)	Simulation time (s)	Average simulation time (s)
12-Bus system	120.74	121.888	126.46	128.612	117.37	118.094
	119.60		127.64		118.28	
	126.43		127.17		117.64	
	122.32		126.88		119.25	
	120.35		134.91		117.93	
15-Bus system	150.83	151.712	164.07	163.824	154.16	151.282
	152.30		163.84		150.24	
	151.52		164.12		150.11	
	151.63		164.30		151.12	
	152.28		162.79		150.78	
33-Bus system	1094.16	1090.088	1143.32	1142.574	1067.12	1067.088
	1095.29		1148.76		1070.34	
	1087.54		1149.11		1066.28	
	1085.59		1134.40		1066.56	
	1087.86		1137.28		1065.14	
69-Bus system	6638.80	6652.97	7050.48	7049.83	6384.94	6526.56
	6659.41		7033.38		6548.74	
	6665.80		7056.70		6622.01	
	6646.73		7051.53		6537.89	
	6654.12		7057.06		6539.22	

Results in Table 10 indicates that better voltage stability condition and lower power loss of the systems can be achieved for active and reactive power supply mode of inverter coupled PV arrays. Changed location and size of PV arrays at lagging and leading 0.95 p.f mode operations in the distribution systems are also presented in Table 10. Maximum improvement of voltage profile at most of the buses can be obtained by 0.95 lagging p.f mode of inverter based PV arrays as shown in Figs. 19–22 for 12-bus, 15-bus, 33-bus and 69-bus, respectively.

There may be less chance of premature convergence in FIPSO and IAPSO because of modification of velocity update formula with information from all neighbors in FIPSO and introduction of diversity factor in position update formula in IAPSO. But, these modifications increase simulation time as shown in Tables 11 and 12.

## 6. Conclusion

This paper has presented a novel multi-objective Particle Swarm Optimization (PSO) based method for optimal placement of wind and solar based Distributed Generation (DG) units into distribution system. The proposed method can comply with voltage and power limit constraints specified by utility. The method targets to improve the voltage stability margin and reduce network power losses utilizing supply from DG units. A new Voltage Stability Factor (VSF) is derived in the study to measure voltage stability level of different buses in the network. VSF is used to quantify voltage stability condition of the whole network also. Comparing with other voltage stability indexes, it can be concluded that developed VSF is very efficient and simple in form. Utilizing performance modeling, optimal location and size selection of Wind Turbine Generation Unit (WTGU) and photovoltaic (PV) array in distribution system are discussed. Optimal placement of inverter interfaced PV arrays and WTGUs have been investigated on 12-bus, 15-bus, 33-bus and 69-bus radial distribution system. Optimal locations and sizes of WTGUs and PV arrays in different distribution systems at maximum penetration level have been identified. It is seen that proposed method performs more efficiently than other DG placement techniques in the context of both power loss minimization and voltage stability improvement of the system. Moreover, WTGUs and PV arrays are considered as both active

and reactive power sources at different power factor (p.f) modes. By analyzing the results it can be concluded that wind and solar based DG in lagging p.f mode causes more enhancement of voltage profile of distribution buses. The results also reveal that voltage magnitudes of the buses rise as penetration of DG increase. Proposed method is very helpful for multiple inverter based DG placement and sizing with static reactive power sources. However, the study can be further extended with dynamic reactive power sources of inverter based DGs.

## Appendix A

### G.1. PSO technique

A set of particles find an optimum through an iterative process in which particles search a space and then adjust their search directions to particle sample near to their fittest neighbor. A swarm of particles are represented as potential solutions, and each particle 'i' is associated with two vectors, i.e., the velocity vector,  $v_i \in \{v_i^1, v_i^2, \dots, v_i^d\}$  and the position vector,  $x_i \in \{x_i^1, x_i^2, \dots, x_i^d\}$ , where d stands for the dimension of the solution space. The velocity and the position of each particle are initialized by random vectors within the corresponding ranges. During optimization search process the velocities and then the positions of the particle are updated as follows:

$$v_i^d = wv_i^d + c_1 \cdot rand_1^d(Pbest_i^d - x_i^d) + c_2 \cdot rand_2^d(Gbest_i^d - x_i^d) \quad (A.1)$$

$$x_i^d = x_i^d + v_i^d \quad (A.2)$$

where  $w$  is the inertia weight and given by

$$w = w_{\max} - \left( \frac{w_{\max} - w_{\min}}{iter_{\max}} \right) iter \quad (A.3)$$

Maximum weight,  $w_{\max}$  and minimum weight,  $w_{\min}$  is set at 0.9 and 0.4, respectively.

$iter_{\max}$  and  $iter$  are the maximum iteration number and current iteration number and are being selected according to the complexity of problem.

$c_1$  and  $c_2$  are the acceleration coefficients.

Here  $rand_1$  and  $rand_2$  are two uniformly distributed random numbers independently generated within  $[0, 1]$  for the  $d$ th dimension.  $Pbest_i$  is the position with the best fitness found so far for the  $i$ th particle, and  $Gbest$  is the best position in the neighborhood.

## References

- [1] Ackermann T, Andersson G, Soder L. Distributed generation: a definition. *Electric Power Syst Res* 2001;57:195–204.
- [2] Acharya N, Mahat P, Mithulananthan N. An analytical approach for DG allocation in primary distribution network. *Int J Electr Power Energy Syst* 2006;28:669–78.
- [3] Singh AK, Parida SK. Combined optimal placement of solar, wind and fuel cell based DGs using AHP. In: Proceedings of world renewable energy congress, Sweden; 2011. p. 3113–20.
- [4] Kashem MA, Ledwich G. Multiple distributed generators for distribution feeder voltage support. *IEEE Trans Energy Convers* 2005;20:676–84.
- [5] Hedayati H, Nabaviniaki SA, Akbarimajid A. A Method for placement of DG units in distribution networks. *IEEE Trans Power Deliv* 2008;23:1620–8.
- [6] Lee SH, Park JW. Selection of optimal location and size of multiple distributed generations by using Kalman filter algorithm. *IEEE Trans Power Syst* 2009;24:1393–400.
- [7] Gonzalez MG, Lopez A, Furado F. Optimization of distributed generation systems using a new discrete PSO and OP. *Electr Power Syst Res* 2012;84:174–80.
- [8] Wang C, Nehrir MH. Analytical approaches for optimal placement of distributed generation sources in power systems. *IEEE Trans Power Syst* 2004;19:2068–76.
- [9] Khatod DK, Pant V, Sharma J. Evolutionary programming based optimal placement of renewable distributed generators. *IEEE Trans Power Syst* 2013;99:1–13.
- [10] Kamel RM, Kermanshahi B. Optimal size and location of distributed generations for minimizing power losses in a primary distribution network. *Trans D Compos Sci Eng Elect Eng* 2009;16:137–44.
- [11] Arya LD, Koshti A, Choube SC. Distributed generation planning using differential evolution accounting voltage stability consideration. *Int J Electr Power Energy Syst* 2012;42:196–207.
- [12] Singh D, Singh D, Verma KS. Multiobjective optimization for DG planning with load models. *IEEE Trans Power Syst* 2009;24:427–36.
- [13] Sedighi M, Igderi A, Parastar A. Siting and sizing of distributed generation in distribution network to improve of several parameters by PSO algorithm. In: Proceedings of international power and energy conference, Singapore; 2010. p. 1083–7.
- [14] Atwa YM, Saadany EF, Salma MAA. Optimal renewable resources mix for distribution system energy loss minimization. *IEEE Trans Power Syst* 2010;25:360–70.
- [15] Gozel T, Hocaoglu MH. An analytical method for the sizing and siting of distributed generators in radial systems. *Electr Power Syst Res* 2009;79:912–8.
- [16] Etehadhi M, Ghasemi H, Zadeh SV. Voltage stability based DG placement in distribution networks. *IEEE Trans Power Deliv* 2013;28:171–8.
- [17] Ugranl F, Karatepe E. Multiple distributed generation planning under load uncertainty and different penetration levels. *Int J Electr Power Energy Syst* 2013;46:132–44.
- [18] Aman MM, Jasmon GB, Mokhlis H, Bakar AHA. Optimal placement and sizing of a DG based on a new power stability index and line losses. *Int J Electr Power Energy Syst* 2012;43:1296–304.
- [19] Injeti SK, Kumar NP. A novel approach to identify optimal access point and capacity of multiple DGs in a small, medium and large scale radial distribution systems. *Int J Electr Power Energy Syst* 2013;45:142–51.
- [20] Ghosh S, Ghoshal SP, Ghosh S. Optimal sizing and placement of distributed generation in a network system. *Int J Electr Power Energy Syst* 2010;32:849–56.
- [21] Ganguly S, Sahoon NC, Das D. Multi-objective particle swarm optimization based on fuzzy-Pareto-dominance for possibilistic planning of electrical distribution systems incorporating distributed generation. *Fuzzy Set Syst* 2013;213:47–73.
- [22] Kumar MVM, Banerjee R. Analysis of isolated power systems for village electrification. *Energy Sust Dev* 2010;14:213–22.
- [23] Aman MM, Jasmon GB, Bakar AHA. Optimum capacitor placement and sizing for distribution system based on an improved voltage stability index. *Int Rev Electr Eng* 2012;7:4622–30.
- [24] Aman MM, Jasmon GB, Bakar AHA, Mokhlis H. A new approach for optimum DG placement and sizing based on voltage stability maximization and minimization of power losses. *J Energy Convers Manage* 2013;70:202–10.
- [25] Jasmon GB, Lee LHC. New contingency ranking technique incorporating a voltage stability criterion. *IEE Proc Gene Trans Distrib* 1993;140:87–90.
- [26] Kashem MA, Ganapathy V, Jasmon GB. Network reconfiguration for enhancement of voltage stability in distribution networks. *IEE Proc Gene Trans Distrib* 2000;147:171–5.
- [27] Shin JR, Kim BS, Park JB, Lee KY. A new optimal routing algorithm for loss minimization and voltage stability improvement in radial power systems. *IEEE Trans Power Syst* 2007;22:648–57.
- [28] Divya KC, Rao PSN. Models for wind turbine generating systems and their application in load flow studies. *Electri Power Syst Res* 2006;76:844–56.
- [29] Wei Z, Hongxing Y, Lin L, Zhaohong F. Optimum design of hybrid solar–wind–diesel power generation system using genetic algorithm. *HKIE Trans* 2007;14:82–9.
- [30] Kennedy J, Eberhart RC. Particle swarm optimization. In: Proceedings of IEEE international conference on neural networks; 1995. p. 1942–8.
- [31] Parsopoulos KE, Vrahatis MN. Multi-objective particle swarm optimization approaches. In: Bui LT, Alam S, editors. (Chapter II) Multi-Objective Optimization in Computational Intelligence. IGI Global; 2008. p. 20–41.
- [32] Jin Y, Olhofer M, Sendhoff B. Dynamic weighted aggregation for evolutionary multi-objective optimization: why does it work and how. In: Proceedings of the genetic and evolutionary computation conference, Morgan Kaufmann; 2001. p. 1042–9.
- [33] Das D, Nagi HS, Kothari DP. Novel method for solving radial distribution networks. *IEE Proc Gene Trans Distrib* 1994;141:291–8.
- [34] Das D, Kothari DP, Kalam A. Simple and efficient method for load flow solution of radial distribution networks. *Int J Electr Power Energy Syst* 1995;17:335–46.
- [35] Baran ME, Wu FF. Network reconfiguration in distribution systems for loss reduction and load balancing. *IEEE Trans Power Deliv* 1989;4:1401–7.
- [36] Baran ME, Wu FF. Optimum sizing of capacitor placed on radial distribution systems. *IEEE Trans Power Deliv* 1989;4:735–43.
- [37] Ellis A, Nelson R, Engeln EV, Walling R, McDowell J, Casey L, Seymour E, Peter W, Barker C, Kirby B. Reactive power interconnection requirements for PV and wind plants – recommendations to NERC, Sandia. Report; 2012. p. 1–39.
- [38] Suresh K, Ghosh S, Kundu D, Sen A, Das S, Abraham A. Inertia adaptive particle swarm optimizer for improved global search. In: 8th International conference on system design and application; 2008. p. 253–8.
- [39] Mendes R, Kennedy J, Neves J. The fully informed particle swarm: simpler, may be better. *IEEE Trans Evol Comput* 2004;8:204–10.
- [40] [http://www.synergysenvirom.com/tools/wind\\_data.asp](http://www.synergysenvirom.com/tools/wind_data.asp).
- [41] Lubosny Z. Wind turbine operation in electric power systems advanced modeling. Verlag: Springer; 2003.
- [42] [http://www.synergysenvirom.com/tools/solar\\_insolation.asp](http://www.synergysenvirom.com/tools/solar_insolation.asp).
- [43] Wei Z, Hongxing Y, Zhaohong F. A novel model for photovoltaic array performance prediction. *Appl Energy* 2007;84:1187–98.